

# The bending-shear-torsion performance of prestressed composite box beam

Hu S. Wei<sup>\*1,2</sup>, Zhao K. Yu<sup>1,2</sup> and Wei C. Jie<sup>1,2</sup>

<sup>1</sup>Department of Materials and Structural Engineering, Nanjing Hydraulic Research Institute, 210029, Nanjing, P.R. China

<sup>2</sup>State Key Laboratory of Hydrology-Water Resources and Hydraulic Engineering, 210098, Nanjing, P.R. China

(Received September 2, 2015, Revised July 18, 2016, Accepted April 8, 2017)

**Abstract.** To study the mechanical performances of prestressed steel-concrete composite box beam under combination of bending-shear-torsion, nine composite beams with different ratio of torsion to bending were designed. Torsion was applied to the free end of the beam with jacks controlled accurately with peripherals, as well as concentrated force on the mid-span with jacks. Based on experimental data and relative theories, mechanical properties of composite beams were analyzed, including torsional angle, deformation and failure patterns. The results showed that under certain ratio of torsion to bending, cracking and ultimate torsion increased and reached to its maximum at the ratio of 2. Three phases of process is also discussed, as well as the conditions of each failure mode.

**Keywords:** prestressed composite box beam; bending-shear-torsion performance; deflection; damage process

## 1 Introduction

Steel-concrete composite beam is a new structure which combined concrete flange and steel beam with steel stud or other shear-resistant connectors. This combination would make full use of their respective mechanical advantages and increase stiffness and carry capacity of this structure. What's more, structure deadweight is reduced; anti-seismic performances, durability and fire resistance are significantly improved. This kind of structure has broad application prospect in architecture.

Torsional performance of composite beam depends on the cooperative work of concrete flange and steel beam. Based on different combinations of torsion and bending, the failure of the structure could be classified as torsional failure, bending failure and torsion-bending failure. Destruction form of structure under torsion-predominate complex loading would be torsional failure, in which oversized shear stress caused by torsion would lead to damage of oblique tension on concrete flange. This loading form of the composite structure makes up space truss system and could be calculated with relative theoretical formulae (Hu *et al.* 2016, Tusnin and Prokic 2015). Meanwhile, pressure stress caused by bending moment would lead to pressure-torsion mix situation inside concrete flange and thus raises the bearing capacity of the structure. Bending failure, which no longer fits space truss system, happened if bending-predominate, while the fracture mode for concrete flange would be shear-pressure mode (Nie *et al.* 2007).

With their own team, Professor Hsu (2009, 2014) and Professor Collins (2013) conducted systematic research on

mechanical performances of composite structures under torsion, shear-torsion or bending-shear-torsion, respectively. Soften-truss model and modified pressure field theory were proposed and formed a good foundation for later research in this field (Ju *et al.* 2013, Mullapudi and Ayoub 2013). Afterwards, based on former models and theories, scholars proposed a variety of improved models. Among the more important are: by dispersing component into elements around the perimeter as well as introducing the plain section assumption along with constitutive relation, balance equation and so on, Onsongo (2007) established equilibrium equations and torsional compatible equations; by decomposing composite structure into bending analysis system based on plain section assumption and torsional analysis system based on pressure field theory, Rahal (2013) established relevant relationship between these two systems through equilibrium equations and torsional compatible correlation. Nie and Hu conducted and analyzed torsional and torsion-bending tests on 8 open-section composite beams and 6 box-section composite beam and proposed calculation system of elastic torsion stiffness, cracking torque and ultimate torque (Hu *et al.* 2016, Nie *et al.* 2004). Lee *et al.* (2010) applied the frequency-dependent spectral element matrix to analysis of bending-shear-torsion coupled composite Timoshenko beams and established relative theoretical model (Lee and Jang 2010). Bernardo *et al.* (2012) improved the variable angle truss model for torsion of reinforced concrete. Most recently, Thivya *et al.* (2016) carried out a set of experiment to study the mechanical behavior of a newly developed composite beam called confined steel concrete composite beam under bending-torsion.

Based on past research, this paper designed a series of prestressed steel-concrete composite box beams under combination of torsion-shear-bending, analyzed testing data combining with relative theory and established some theoretical results. Before this article, researches on this

---

\*Corresponding author, Professor  
E-mail: [xqfan@nhri.cn](mailto:xqfan@nhri.cn)

specific structure are rare and uncompleted.

steel structure and GB 50010-2010 (2010), Code for design of concrete structure.

## 2 Experiment introductions

### 2.1 Model design and production

Taking into account engineering requirement and relevant provisions of the current codes (steel girders were designed based on code for design of steel structure, while concrete flanges were designed based on code for concrete structure), nine prestressed steel-concrete composite box beams were designed and numbered PCB-51 and PCB-54~61. Made from ML15 (cold heading steel), studs were uniformly arranged double-row along lengthwise direction. Taking account of factors like available space inside lab, equipment conditions and shear lag effect, clear spans of composite box girders was designed to be 3 m long, 0.39 m high, 0.8 m wide. The effective width of concrete flange thickness obtained by calculating is 0.13 m ( $b_c/h_c > 6$ ). To protect girders, made from high strength concrete (C60), from unexpected damages, flanges were added at 500 mm from edge on both sides and stirrups were doubled. Steel beams, made of Q235-B, whose sizes and details are shown in Fig. 1. Basic parameters of each of the 9 girders are shown in Table 1, and loading parameters Table 2. Main material parameters are shown in Table 3 - Table 5. Concrete and steel adopted in this experiment is designed based on GB 50017-2003 (2003), Code for design of

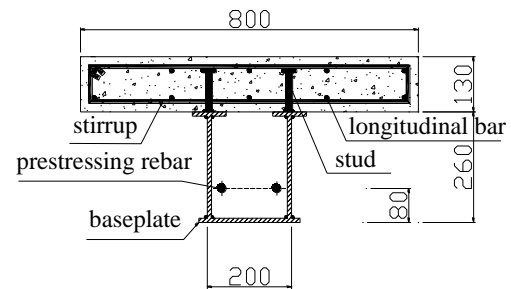


Fig. 1 Section Size of Beam (Unit: mm)



Fig. 2 Welding Studs

Table 1 Section parameters and reinforcements

| number              | cross-section size<br>(mm×mm) |          | prestressed<br>tendon | rebar        |              | Span<br>(mm) | Number of<br>studs | Longitudinal<br>spacing<br>(mm) | Comment           |
|---------------------|-------------------------------|----------|-----------------------|--------------|--------------|--------------|--------------------|---------------------------------|-------------------|
|                     | Steel girder                  | Concrete |                       | lengthwise   | stirrup      |              |                    |                                 |                   |
| PCB-51<br>PCB-54~60 | 200×260                       | 800×130  | 2 $\phi^j$ 15.24      | 10 $\phi$ 10 | $\phi$ 8@120 | 3000         | 76                 | 85                              | Standard          |
| PCB-61              | 200×260                       | 800×130  | 2 $\phi^j$ 15.24      | 10 $\phi$ 10 | $\phi$ 8@120 | 3900         | 76                 | 85                              | Span<br>increased |

Table 2 Main loading parameters and reinforcement ratio

| number | Prestress<br>(kN) | tension strain of<br>prestressing tendons<br>( $\times 10^{-6}$ ) | Stirrup ratio<br>(%) | Longitudinal<br>rebar ratio | Prestressed<br>reinforcement index<br>(%) | Loading mode          | Torque/Bending<br>$\frac{T/T_u}{M/M_u}$ |
|--------|-------------------|---|----------------------|-----------------------------|---|-----------------------|---|
| PCB-51 | 168.2             | 34  | 0.68                 | 0.75%                       | 1.22                                      | torsion               |   |
| PCB-54 | 177.6             | 34  | 0.68                 | 0.75%                       | 1.22                                      | bending-shear-torsion | 2                                       |
| PCB-55 | 169.2             | 40  | 0.68                 | 0.75%                       | 1.22                                      | bending-shear         | 0                                       |
| PCB56  | 174.0             | 38  | 0.68                 | 0.75%                       | 1.22                                      | bending-shear-torsion | 5                                       |
| PCB-57 | 189.6             | 36  | 0.68                 | 0.75%                       | 1.22                                      | bending-shear-torsion | 1                                       |
| PCB-58 | 168.2             | 36  | 0.68                 | 0.75%                       | 1.22                                      | bending-shear-torsion | 0.5                                     |
| PCB-59 | 188.4             | 31  | 0.68                 | 0.75%                       | 1.22                                      | bending-shear-torsion | 3.5                                     |
| PCB-60 | 181.9             | 26  | 0.68                 | 0.75%                       | 1.22                                      | bending-shear-torsion | 6.5                                     |
| PCB-61 | 208.0             | 40  | 0.68                 | 0.75%                       | 1.22                                      | bending-shear-torsion | 1                                       |

Table 3 Mechanic property parameters of steel beam

| Type                                       | Material | $E_s / \text{MPa}$ | $\varepsilon_y / 10^{-6}$ | $f_y / \text{MPa}$ | $f_u / \text{MPa}$ |
|--|----------|--------------------|---------------------------|--------------------|--------------------|
| Web plate,<br>Layer board<br>and baseboard | Q235B    | $20.6 \times 10^4$ | 1383                      | 285                | 435                |

Table 4 Mechanic property parameters of prestressed tendons and bars

| Type               | Diameter (mm) | Area (mm <sup>2</sup> ) | $E_s / \text{MPa}$ | $\varepsilon_y / 10^{-6}$ | $f_y / \text{MPa}$ | $f_u / \text{MPa}$ |
|--------------------|---------------|-------------------------|--------------------|---------------------------|--------------------|--------------------|
| Longitudinal bar   | 10            | 78.5                    | $20.6 \times 10^4$ | 1214                      | 250                | 385                |
| Stirrup            | 10            | 78.5                    | $20.6 \times 10^4$ | 1190                      | 245                | 380                |
| Prestressed tendon | 15.2          | 139                     | $19.5 \times 10^4$ | 7153                      | 1395               | 1860               |

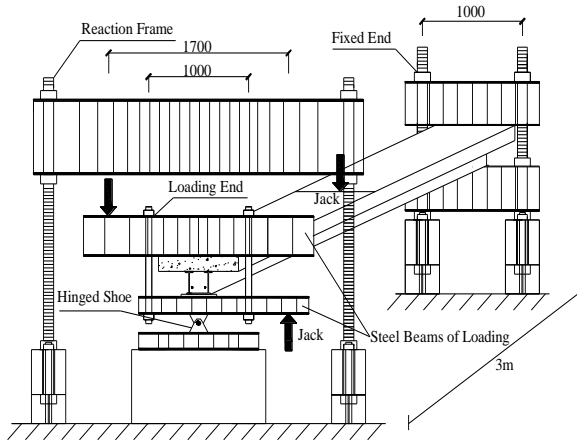


Fig. 3 Test loading system



Fig. 4 The test device

## 2.2 Test facility and loading scheme

In this experiment, one end of the beams was fixed with steel beam and the torque was applied in the other one. On the load-end, an 8-channel high-precision hydraulic servo loading-system was outfitted to apply bilateral eccentric concentrated forces which served as torque. With concentrated  $\phi^j$  force applied to the mid-span of the beam at the same time, the beams were at a bending-shear-torsion condition. Post-tensioned method was used to apply prestress to two  $\phi^j$  15.2 bars with 3-ramp loading, and the strength of the strings was 1860 MPa. During the loading process, tests were performed under loading control carried out accurately with attached computer control system shown in Fig. 3.

This experiment adopted prestressed reinforced concrete composite box girders span 2 m, the key steps were as follows:

- 1) Set force sensors and get torsion applied.
  - 2) Plaster two different kinds of strain gauges (BF120-3AA, BF120-80AA) to measure strain of mid-span and collect data with static strain acquisition instrument DH3816 made by Dong-Hua company.
  - 3) Apply electronic angle gauges (accuracy of 0.01°) to edge of girders.
  - 4) Set electronic displacement meters to carry out deflection measurement of the girder while loading.
  - 5) Observe propagation of crack on the concrete flange.
- Before loading, prestress is 3-stage stretched until 25 MPa, values of prestress and strain are collected after each stage of stretching. To prevent inner-force instability while loading, values are collected after 5 min static loading at each loading stage. Specific loading conditions of this experiment are as follow:

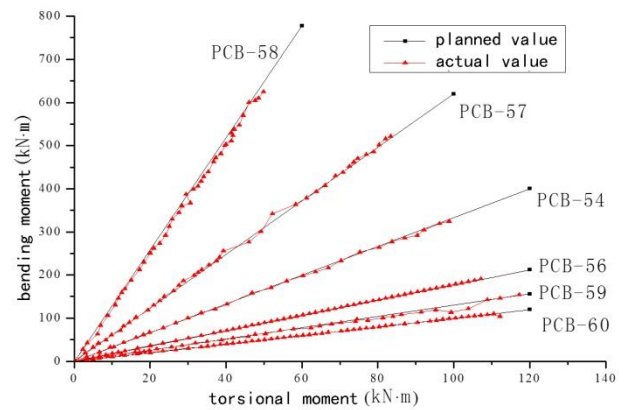


Fig. 5 Loading conditions

Table 5 Mechanical property parameters of concrete

| Group number | $f_{cu,150} (\text{MPa})$ | $f_{tk} (\text{MPa})$ | $f_{ck} (\text{MPa})$ | $E_c (\text{MPa})$ | $G_c (\text{MPa})$ | $\varepsilon_{tp} (10^{-6})$ | $\varepsilon_{lp} (10^{-6})$ |
|--------------|---------------------------|-----------------------|-----------------------|--------------------|--------------------|------------------------------|------------------------------|
| Group 1      | 66.9                      | 58.4                  | 3.1                   | $3.6 \times 10^4$  | $1.68 \times 10^4$ | 140                          | 297                          |
| Group 2      | 66.7                      | 58.2                  | 3.1                   | $3.6 \times 10^4$  | $1.68 \times 10^4$ | 139                          | 292                          |
| Group 3      | 68.2                      | 58.9                  | 3.1                   | $3.6 \times 10^4$  | $1.68 \times 10^4$ | 148                          | 312                          |
| Average      | 67.8                      | 58.6                  | 3.1                   | $3.6 \times 10^4$  | $1.68 \times 10^4$ | 144                          | 300                          |

### 3 Experiment results analyses

#### 3.1 Experimental phenomena and failure mode

Two failure modes were discovered in the experiments.

##### (1) Torsional failure mode

Torsional failure is the main failure mode when composite beam is under combination of loads with ratio of torsion to bending being fairly larger ( $T/T_u/M/M_u=2, 3.5, 5, 6.5$ ). When it comes to the cracking stage, tiny inclined cracks begin to appear and expand until run through and form spiral cracks. Stirrups yield when concrete flange fail. Of the whole process, longitudinal bars are under tension, the failure statue of composite beam under torsion-predominate complex loading is similar to that of pure torsion. Diagrams of failure characteristics are shown in Fig. 6~Fig. 7.

##### (2) Bending failure mode

Bending failure is the main failure mode when composite beam is under combination of loads with ratio of torsion to bending being fairly small ( $T/T_u/M/M_u=0, 0.5, 1$ ). When beam damages in bending failure, crushing happened in top of concrete flange while all longitudinal bars yield. In the loading process, horizontal cracks firstly appear on location of bottom of concrete flange correspond to the loading point, moreover, concrete flange enters into cracking stage, bottom area of steel beam begin to yield, neutral axis moves upward. Along with the load increasing, horizontal cracks appears quickly while width of which increases, deflection of mid-span increases faster as well. Finally with neutral axis moving upward, compressive zone of concrete flange decreases, maximum crack expands

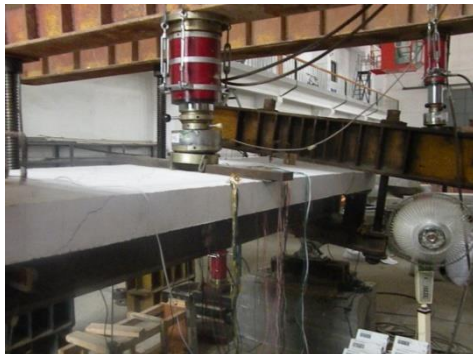


Fig. 6 Torsional failure of beam



Fig. 7 Cracks on top of beam



Fig. 8 Bending failure of beam



Fig. 9 Cracks of bending failure

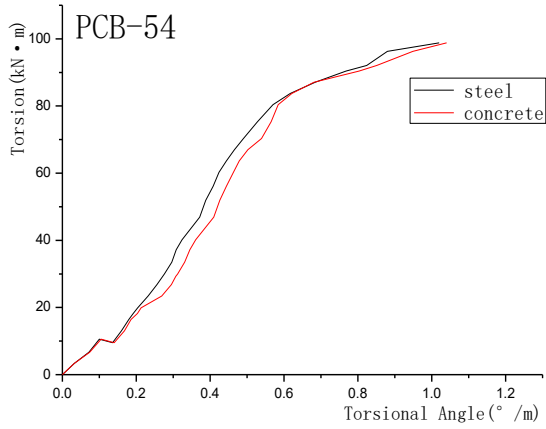
rapidly and from which concrete crushes and causes the failure of the whole composite beam. Diagrams of failure characteristics are shown in Fig. 8~Fig. 9.

#### 3.2 Torque and torsional angle

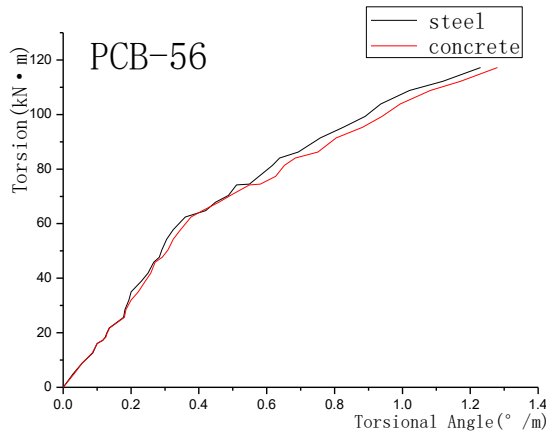
Considering that the torsional angles of concrete flange and steel beam are roughly equal, it is reasonable to assume that they work together. Since the steel beam is closer to the torsion center than concrete flange, the torsion angle of concrete flange is slightly bigger than that of the steel beam.

The process could be divided into three phases: elastic stage, cracking stage and failure stage. In the elastic stage, deformation of the composite beam is basically in agreement with the linear elastic criteria; in the second stage, series of approximately parallel inclined cracks began to appear and slowly expanded; when it reached to the damage stage, cracks began to expand sharply instead of increase in number, surface of the concrete flange was beginning to husk out and come off, deformation increased to damage level and the whole composite beam reached to the ultimate torque. All over the process, no separation happened between concrete flange and steel beam.

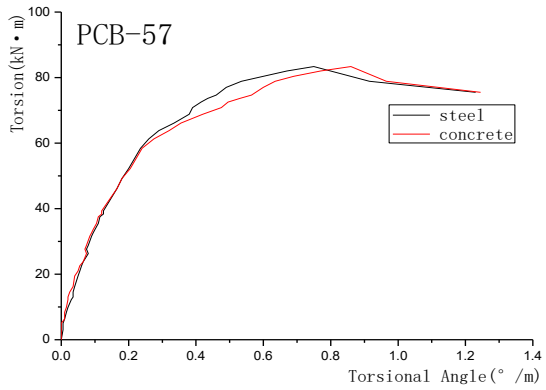
Relation curves of four representative tests are shown in Fig. 10, it can be seen that stiffness starts to diminish after cracking. The bigger the ratio between torsion and bend is, the more sharply the torsional stiffness of beams will decrease. A range of bending moment helps with the torsional strength.



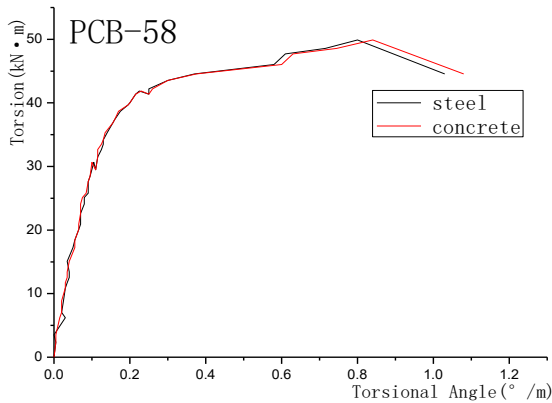
(a) PCB-54



(b) PCB-56

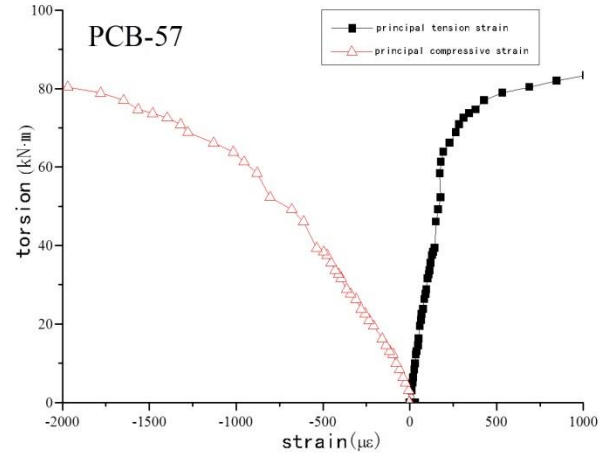


(c) PCB-57

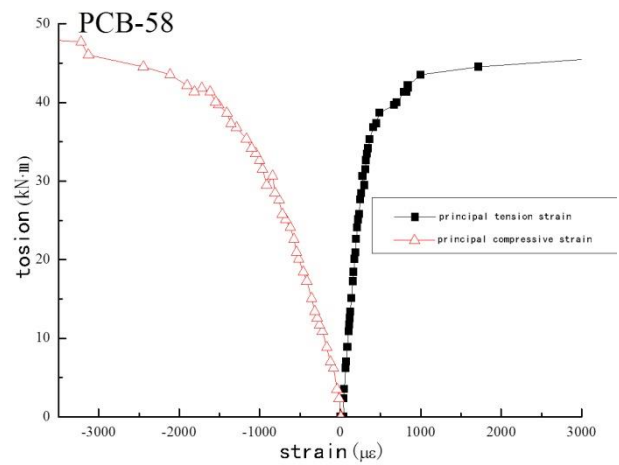


(d) PCB-58

Fig. 10 Torque-Angle of Torsion Curves



(a) PCB-57



(b) PCB-58

Fig. 11 Strain of concrete flange

### 3.3 Concrete strain distribution

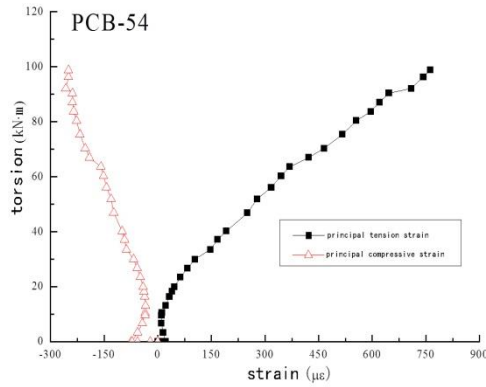
Strain of concrete parts of composite beams under combination of bending-shear-torsion is shown in Fig. 11.

Due to pre-stress applied on steel beam, composite box beam generates counter-arched effect and top of concrete flange is under longitudinal tension state. Before torsion of composite beam reached  $0.5T_u$ , concrete flange is within elastic stage, also, principal tension strain and compressive strain are quasi-linearly related. When it goes into the cracking stage, both principal tension strain and compressive strain begin to increase significantly.

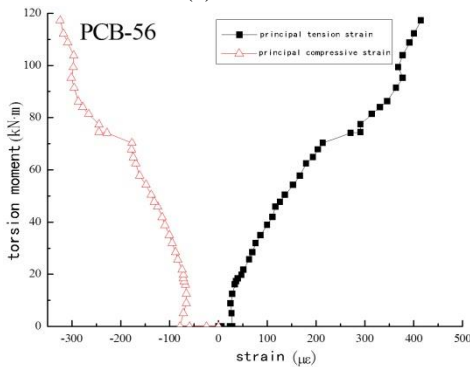
Response to bending moments of whole process, beam is mainly subjected to compressive stress. The smaller the ratio of torsion to bending, the bigger the difference between principal compressive stress and principal tension stress, also, the bigger the angle between inclined cracks of flange and vertical axis.

### 3.4 Steel beam strain distribution

Strain of steel parts of prestressed composite beam under bending-shear-torsion combination is shown as follows:

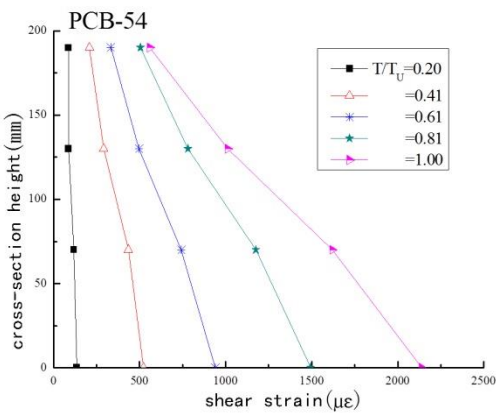


(a) PCB-54

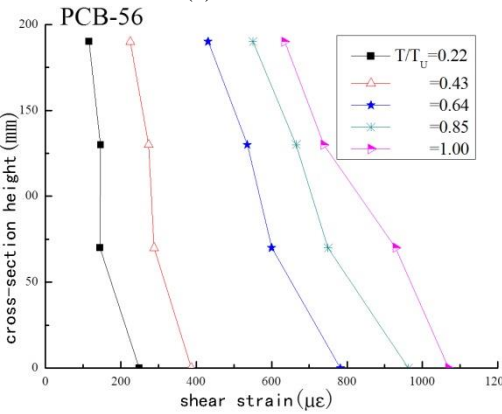


(b) PCB-56

Fig. 12 Strain of Steel Beam



(a) PCB-54



(b) PCB-56

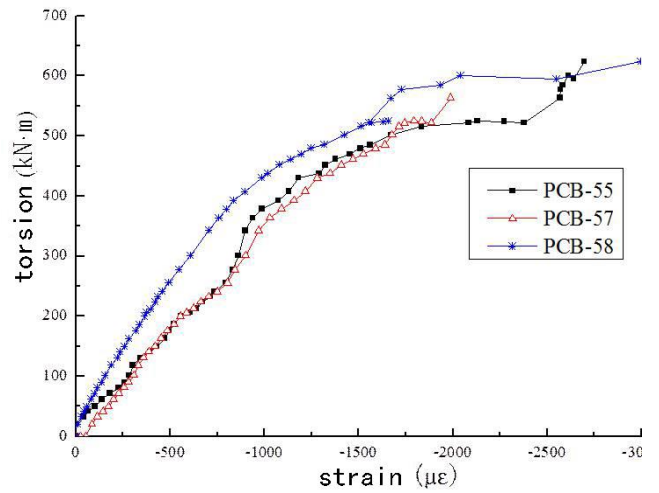
Fig. 13 Shear Strain of Steel Beam

Under bending-shear-torsion combination, principal tension stress of steel beam is larger than principal compressive stress. The smaller the ratio of torsion to bending is, the larger the difference between principal tension strain and compressive strain will be. Due to tension stress generated by bending moments, steel beam is under tension-torsion state, of which the principal tension stress when broken is larger than that under torsion only.

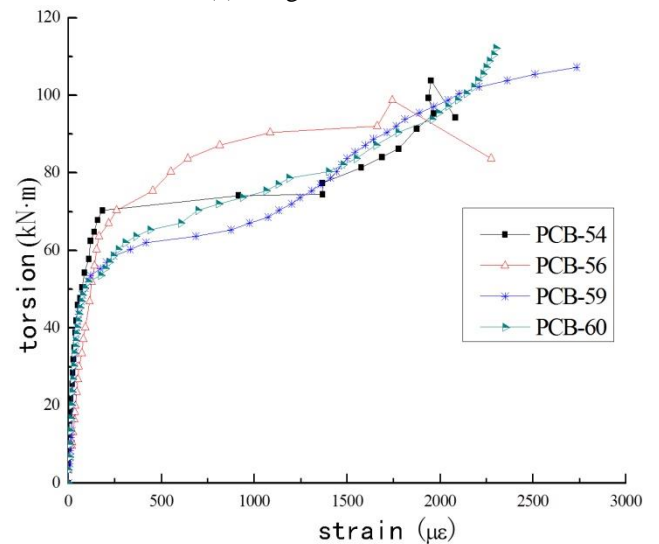
Shear stress of steel box increases gradually along the cross from top to the bottom and demonstrates linear change.

### 3.5 strain of steel bar

Strain of steel bars inside prestressed composite beam is shown as follows:



(a) Longitudinal Bars



(b) Stirrups

Fig. 14 Shear Strain of Steel Bars

In the bending damage mode, strain of longitudinal bars increases quasi-linearly with bending moment, also, longitudinal bars is under compressive situation and the maximum compressive strain is smaller than that of pure bending situation. As for the torsional damage mode, longitudinal bars is basically under tensional situation but not yielded.

In the torsional damage mode, strain of stirrup is relatively small of about  $250 \mu\epsilon$  when  $T < 0.7T_u$ . When  $T > 0.7T_u$ , strain began to increase faster until yield of stirrups. Under effect of torsion moment, stirrups undergo a large plastic deformation.

### 3.6 Bending-deflection curve

As shown in Fig. 15, bending moment of the beam is closely related to the deflection and correlation reflects differently in each of the three phases. In the elastic stage, flexural and torsional rigidity of the beams remains unchanged, bending moment and deflection are linear associated. With the continuous increasing of bending moment till the beam reaches the crack stage, traverse cracks are beginning to appear on the bottom of the concrete flange and steel girder begin to yield, meanwhile, bending moment and deflection are no longer linearly relevant. With further increase of loads, steel plate and web yield, cracks widens, neutral axis go higher, bending stiffness fall sharply and it come into the damage stage. In this stage, deflection continues increasing despite loads remains the same, mid-span deflection reaches to about 1.03%~1.67% of the clear span, ductility in bending performs well.

The bigger the ratio between moments of torsion and bending, the greater the mid-span deflection of beam under same loads, as well as the ductility.

### 3.7 Torsion-bending moment curve

Fig. 16 shows the relation curve of torsion and bending moments. Under the influence of combination of bending-shear-torsion, when ratio of torsion to bending is larger than 2, the torsional strength of the beam increases, which reveals the phenomena that certain moment could enhance the ultimate torsional strength. The ultimate torsional strength reaches a maximum of 114% when the ratio reaches 5:1 (PCB-56), and then starts to decline; when ratio of torsion to bending is lower than 2, ultimate torsional strength reduced rapidly and the bending failure serves as the main damage mode.

Under the influence of combination of bending-shear-torsion, mechanical behavior of steel-concrete composite beams is different from normal reinforced ones. With proper moment, the ultimate torsional strength could be improved. Torsion in composite beams is mainly borne by concrete flange and steel girder, and torsional damages are mainly marked by the instability of the concrete flange. Under certain moments, concrete flange is mainly in compression situation, bending stress generated by the bending moment partly counteracted diagonal tension caused by the torque, thus suppressed the propagation of

inclined cracks.

### 3.8 Section stress analysis

Fig. 17 shows the section stress of beam in yield bending damage. Because of arch effect caused by prestress, concrete flange is in tensional situation while steel beam in compression. Before yielding of the composite beam, the bending strain largely matched the assumption that the section is plane. Neutral axis is above the interface and near the lower longitudinal bar. Because of the prestress, the elastic range of the beam is expanded, flexural stiffness and cracking moment increased, what's more, crack propagation is restrained.

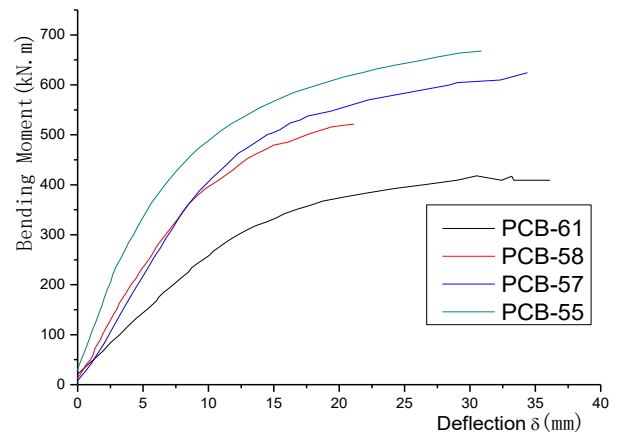


Fig. 15 Moment-midspan deflection curve

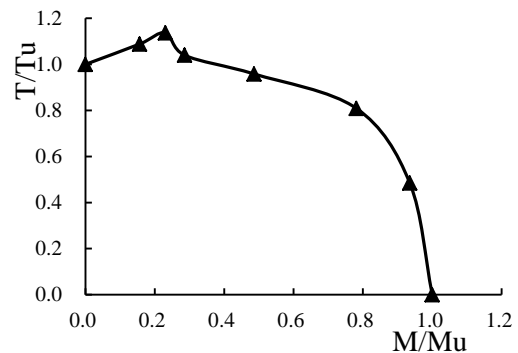
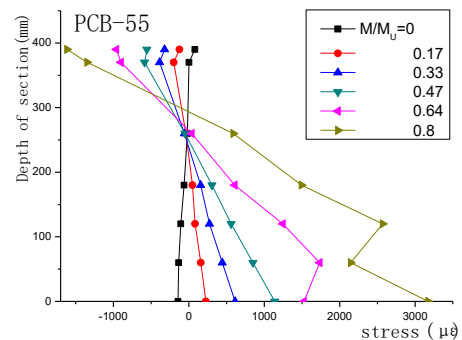


Fig. 16 Torsion-bending moment curve



(a) PCB-55

Fig. 17 Stress along the Height

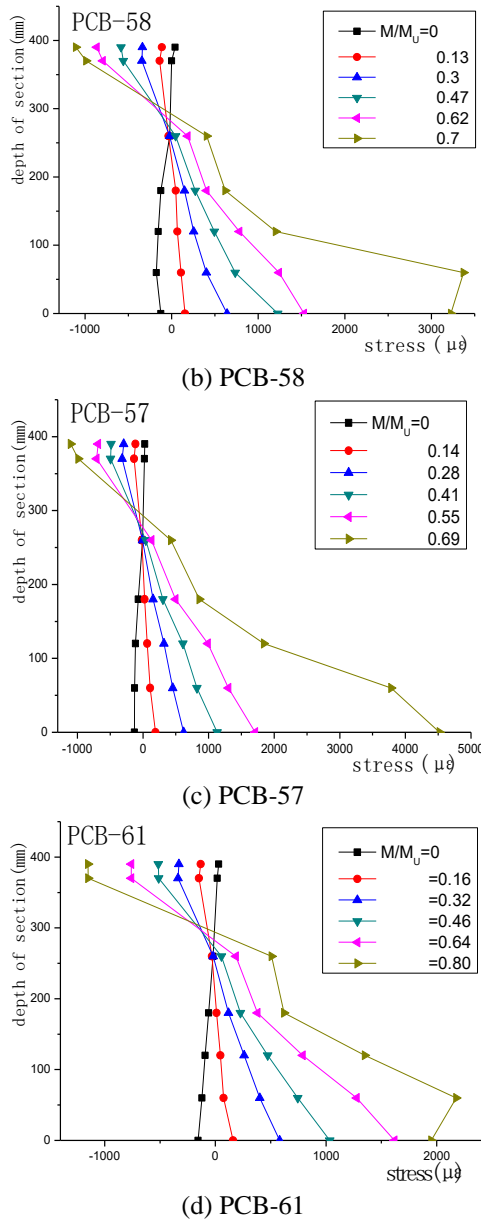


Fig. 17 Continued

Along with beam going into the yield stage, growth of section strain is becoming less regularly. Stress of the bottom significantly increases and causes the bottom part to reach yield phase even earlier. Beams are able to bear more after steel beam yields, which is due to good ductility of steel and reinforcement of prestress.

#### 4. Correlation analysis of bending-shear-torsion

With ratio of torsion to bending being large, failure mode of composite beam under combination of bending-shear-torsion is similar to the third failure mode of reinforced concrete member (status III), which manifests as the yield of steel bars inside the concrete flange and plastic compression of lower side walls; with ratio being small, the failure mode is similar to the first failure mode of reinforced

concrete member (status I), manifests as plastic compression of upper side walls. Relative formulae of composite box beam under bending-shear-torsion could be as follows (Barry *et al.* 2011, Rizov and Miadensky 2012).

Torsional failure (status III)

$$\left(\frac{T}{T_u}\right)^2 + \left(\frac{V}{V_u}\right)^2 + \frac{M}{M_u} \left(-\frac{1}{r}\right) = 1 \quad (1)$$

Flexural failure (status I)

$$\left(\frac{T}{T_u}\right)^2 r + \left(\frac{V}{V_u}\right)^2 r + \frac{M}{M_u} = 1 \quad (2)$$

$T_u$  stands for the ultimate torsion of composite beam under torsion;  $V_u$  stands for the ultimate shear of composite beam under torsion;  $M_u$  stands for the ultimate bending of composite beam under torsion.

Value of  $r$  could be obtained by substituting the test data into formulae (1) and (2):

Torsional failure (status III)

$$\left(\frac{T}{T_u}\right)^2 + \left(\frac{V}{V_u}\right)^2 - 1.24 \frac{M}{M_u} = 1 \quad (3)$$

Flexural failure (status I)

$$0.48 \left(\frac{T}{T_u}\right)^2 + 0.48 \left(\frac{V}{V_u}\right)^2 + \frac{M}{M_u} = 1 \quad (4)$$

Under certain bending moments, the concrete flange is in the compression situation, positive bending stress generated by bending moments counteracts the part of the oblique torsional stress generated by torsion (Wan and Mahendran 2015). Thus suppresses the expansion of cracks and the ultimate torsion of composite beam is increased. It is also reasonable to regard the composite beam as an asymmetry prestressed concrete member, in this case, steel beam could be treated like longitudinal bars and reinforced concrete flange as asymmetry reinforcement distribution mode, then the relative curve of moments obeys the parabolic law

$$\frac{M}{M_u} = a \left(\frac{T}{T_u}\right)^2 + b \left(\frac{V}{V_u}\right)^2 + c \frac{T}{T_u} + d \frac{V}{V_u} + e \quad (5)$$

Put test data into equations and we could get values of  $a$ ,  $b$ ,  $c$ ,  $d$ ,  $e$ . Given that  $V$  in this experiment is much less than ultimate shear  $V_m$ , it is reasonable to define  $b=0$  and  $d=0$ , so to simplify the equation.

For torsional damage

When  $M < 0.24M_u$ ,

$$\frac{M}{M_u} = -1.6873 \left(\frac{T}{T_u}\right)^2 - 5.2926 \frac{T}{T_u} - 3.6053 \quad (6)$$

For bending damage

When  $0.24M_u < M < M_u$ ,

$$\frac{M}{M_u} = -0.9365 \left(\frac{T}{T_u}\right)^2 + 0.4105 \frac{T}{T_u} + 0.9928 \quad (7)$$

## 5. Conclusions

In this article, 9 steel-concrete composite beams under different combination of bending-shear-torsion were designed to obtain the impact of ratio of torsion to bending on section stress, deflection, torsion angle and so on. Based on former analysis, we could draw conclusions as follows:

1) When  $T/T_u/M/M_u \leq 1$ , bending moment played important role in the damage process which could be defined as bending damage and the failure was marked by compression failure of concrete flange and rapid increase of mid-span deflection. When  $T/T_u/M/M_u > 1$ , the beam was mainly under the impact of torsion and the damage mode is torsional damage. After failure of the beam, most of the longitudinal bars and stirrups yielded.

2) Bending moment of certain values enhanced the cracking torsion and ultimate torsion and restricted the emergence and propagation of inclined cracks upon the surface. Within certain range, torsional stiffness and ultimate torque increased with ratio between torsion and bending. In this experiment, when  $T/T_u/M/M_u > 2$ , the ultimate torsion increased with the value of  $T/T_u/M/M_u$ , until it reached 5 while the ultimate torsion increased 14%. When  $T/T_u/M/M_u < 2$ , ultimate torque of composite beam decreased in different degree.

3) Before yielding of steel girder, beam was basically in line with the plan section assumption, when it came into the yield stage, beams no longer met the assumption. The mid-span deflection improved significantly while the ratio between torsion and bending remained small and hence enhanced the bending ductility. The bending stiffness of beam increased with decrease of ratio.

In this article, theoretical study of prestressed steel-concrete composite beam under bending-shear-torsion was conducted, correlative formulae were deduced, and experimental data was processed and analyzed. Data and formulae acquired in this article is a complement to the correlation domain theory and practice.

## Acknowledgements

This study was funded by China National Funds for Distinguished Young Scientists(No.51325904), National Natural Science Foundation of China (No.51527811, 51679150), The National Key Research and Development Program of China (No.2016YFC0401902). Thanks for the helps.

## References

- Bernardo, L.F.A., Andrade, J.M.A. and Lopes, S.M.R. (2012), "Modified variable angle truss-model for torsion in reinforced concrete beams", *Mater. Struct.*, **45**(12), 1877-1902.
- Davidson, B.D. and Felipe O. Sediles (2011), "Mixed-mode I-II-III delamination toughness determination via a shear-torsion-bending test", *Compos. Part A: Appl. Sci. Manufact.*, **43**(6), 589-603.
- Hu, S.W., Zhao, K.Y. and Yu, J. (2016), "Whole process of

- prestressed steel-concrete composite box beam under bending-torsion[J]", *Sichuan Build. Sci.*, **42**(3), 1-6.
- Jeng, C. and Hsu, T.T.C. (2009), "A softened membrane model for torsion in reinforced concrete members", *Eng. Struct.*, **31**(9), 1944-1954.
- Ju, H., Lee, D.H., Hwang, J.H., Kang, J.W., Kim, K.S. and Oh, Y.H. (2013), "Torsional behavior model of steel-fiber-reinforced concrete members modifying fixed-angle softend-truss model", *Compos. Part B:Eng.*, **45**(1), 215-231.
- Kuo, W.W. and Hsu, T.T.C. (2014), "Hwang Shyh Jiann, Shear strength of reinforced concrete beams", *ACI Struct. J.*, **111**(4), 809-818.
- Lee, U. and Jang, I.J. (2010), "Spectral element model for axially loaded bending-shear-torsion coupled composite Timoshenko beams", *Compos. Struct.*, **92**(12), 2860-2870.
- Mihaylov Boyan, I., Bentz Evan, C. and Collions Micheal P. (2013), "Two-parameter kinematic theory for shear behavior of deep beams[J]", *ACI Struct. J.*, **110**(3), 447-455.
- Mullapudi, T.R.S. and Ashraf Ayoub (2013), "Analysis of reinforced concrete columns subjected to combined axial, flexure, shear and torsional loads", *J. Struct. Eng.*, **139**(4), 561-573.
- Nie, J.G., Xiao, Y. and Che, L. (2004), "Experimental studies on shear strength of composite steel-concrete beams", *J. Struct. Eng.*, ASCE, **130**(8), 1206-1213.
- Nie, J.G., Cai, C.S., Zhou, T.R. and Li, Y. (2007), "Experimental and analytical study of prestressed steel-concrete composite beams considering slip effect", *J. Struct. Eng.*, **133**(4), 530-540.
- Onsongo, W.M. (2007), "Failure interaction curves for combined loading involving torsion, bending and axial loading", *J. South African Inst. Civ. Eng.*, **49**(1), 17-24.
- Rahal, K.N. (2013), "Torsional strength of normal and high strength reinforced concrete beams", *Eng. Struct.*, **56**(10), 2206-2216.
- Rizov, V. and Miadensky, A. (2012), "Analysis of mode II crack in bilayered composite beam", *J. Theo. Appl. Mech.*, **42**(2), 67-78.
- Thivya, J., Malathy, R. and Tensing, D. (2016), "Behavior of composite beams under combined bending and torsion[J]", *Int. J. Adv. Eng. Technol.*, **563**(2), 563-566.
- Tusnin, A.R. and Milan Prokic (2015), "Selection of parameters for I-beam experimental model subjected to bending and torsion", *Procedia Eng.*, **111**(7), 789-796.
- Wan, H.X. and Mahendran, M. (2015), "Bending and torsion of hollow flange channel beams", *Eng. Struct.*, **84**(2), 300-312.

CC